

## Demonstration of a 1/4-Cycle Phase Shift in the Radiation-Induced Oscillatory Magnetoresistance in GaAs/AlGaAs Devices

R. G. Mani,<sup>1</sup> J. H. Smet,<sup>2</sup> K. von Klitzing,<sup>2</sup> V. Narayanamurti,<sup>1,3</sup> W. B. Johnson,<sup>4</sup> and V. Umansky<sup>5</sup>

<sup>1</sup>*Gordon McKay Laboratory of Applied Science, Harvard University, 9 Oxford Street, Cambridge, Massachusetts 02138, USA*

<sup>2</sup>*Max-Planck-Institut für Festkörperforschung, Heisenbergstrasse 1, 70569 Stuttgart, Germany*

<sup>3</sup>*Harvard University, 217 Pierce Hall, 29 Oxford Street, Cambridge, Massachusetts 02138, USA*

<sup>4</sup>*Laboratory for Physical Sciences, University of Maryland, College Park, Maryland 20740, USA*

<sup>5</sup>*Braun Center for Submicron Research, Weizmann Institute, Rehovot 76100, Israel*

(Received 25 September 2003; published 8 April 2004)

We examine the phase and the period of the radiation-induced oscillatory magnetoresistance in GaAs/AlGaAs devices utilizing *in situ* magnetic field calibration by electron spin resonance of diphenyl-picryl-hydrazal. The results confirm a  $f$ -independent 1/4-cycle phase shift with respect to the  $hf = j\hbar\omega_c$  condition for  $j \geq 1$ , and they also suggest a small ( $\approx 2\%$ ) reduction in the effective mass ratio,  $m^*/m$ , with respect to the standard value for GaAs/AlGaAs devices.

DOI: 10.1103/PhysRevLett.92.146801

PACS numbers: 73.21.-b, 73.40.-c, 73.43.-f

Measurements [1] of GaAs/AlGaAs devices including a two-dimensional electron system (2DES) have recently shown that vanishing resistance can be induced by photoexcitation at liquid helium temperatures, in a weak-magnetic-field large-filling-factor limit [1–3]. The possibility of identifying a new physical mechanism for inducing vanishing resistance in the 2DES has motivated much theoretical interest in this phenomenon [4–9], which shares features of the zero-resistance states in the quantum Hall situation, minus Hall quantization [10,11].

Experiments suggest that this novel effect is characterized, in the Hall geometry, by a wide magnetic field,  $B$ , interval where the diagonal resistance,  $R_{xx}$ , becomes exponentially small upon photoexcitation in the low temperature,  $T$ , limit [1,2,12]. Measurements have also indicated that increasing the radiation frequency,  $f$ , linearly shifts distinguishing features to higher  $B$  [13,14]. Thus, one might define from  $f$  a field scale  $B_f = 2\pi f m^*/e$ , where  $e$  is the electron charge, and  $m^*$  is an effective mass [1]. According to theory, the observed periodicity reflects the interplay between the photon energy,  $hf$ , and integral ( $j$ ) cyclotron energies,  $j\hbar\omega_c$ , and  $B_f$  is defined by  $hf = \hbar\omega_c$  [4,6,8]. Hence, in the expression for  $B_f$ ,  $e$  is a known constant,  $f$  can be measured accurately, and  $m^*$  can be taken, initially, to be the standard value for  $m^*$  in GaAs/AlGaAs, although it could involve corrections.

A problem of interest is to identify the  $B$  intervals that exhibit vanishing resistance at a fixed  $f$ , and to connect them in a simple way to  $B_f$  because the relation between the two scales ( $hf$ ,  $j\hbar\omega_c$ ), which is set by  $B$ , is likely to be essential in the underlying physics. In earlier work, we had reported that resistance minima occur about  $B = [4/(4j+1)]B_f$  and resistance maxima transpire about  $B = [4/(4j+3)]B_f$ , with  $j = 1, 2, 3 \dots$  [1]. This “minima about  $B = [4/(4j+1)]B_f$ ” result might also be loosely reformulated as a “1/4-cycle phase shift” with respect to the  $hf = j\hbar\omega_c$  condition [15].

Our minima about the  $B = [4/(4j+1)]B_f$  result seems incongruent, however, with a report which identified radiation-induced resistance minima with  $\omega/\omega_c = j + 1/2$ , i.e.,  $B_f/B = j + 1/2$ , and resistance maxima with  $\omega/\omega_c = j$ , i.e.,  $B_f/B = j$ , where  $\omega = 2\pi f$  [14]. Briefly, that study of low mobility specimens exhibited  $T$ -insensitive  $R_{xx}$  oscillations, a large nonvanishing resistance at the minima even at the lowest  $T$ , and the absence of a phase shift [14]. A subsequent study of high mobility specimens identified resistance maxima with  $\omega/\omega_c = j$ , as it placed resistance minima on the high magnetic field side of  $\omega/\omega_c = j + 1/2$  [2].

A recent reformulation [16] asserts that the phase of the  $R_{xx}$  oscillations in Ref. [2] are consistent with a 1/4-cycle phase shift [1], but only at low- $B$ , i.e.,  $j \geq 4$ . Although this reinterpretation has helped to bring overlap between theory [4,6,8] and recent experiment [1,2,12,13,16], there continues to be a phase variance in the regime of low  $j$ ,  $j \leq 4$ , between our initial report announcing these novel zero-resistance states and the report by Zudov *et al.*, confirming the same [1,2].

Phase characterization in this context requires an accurate measurement of  $B$  since the observed oscillations are referenced to  $f$ , which sets  $B_f$ . In the laboratory, the transport setup typically includes a high-field superconducting magnet, and  $B$  is often determined from the magnet coil current,  $I$ , via a calibration constant. At low  $B$ ,  $B \leq 0.5$  T, this approach to  $B$  measurement can be unreliable due to nonlinearity and hysteresis in the  $B - I$  characteristics of the field coil, and  $B$  offsets due to trapped flux and/or current offsets in the magnet power supply. An *in situ* Hall probe can be applied to correct this problem. However, even this approach is prone to field measurement errors arising from misalignment voltages in the Hall sensor or changes in the Hall constant [17]. To reduce such uncertainties, we have carried out microwave transport studies of the 2DES with *in situ*  $B$ -field calibration by electron spin resonance (ESR) of

diphenyl-picryl-hydrazal (DPPH). The results demonstrate a  $f$ -independent  $1/4$ -cycle phase shift in the radiation-induced oscillatory magnetoresistance, and they suggest a small reduction in the mass ratio characterizing this phenomena, with respect to the standard value for  $m^*/m$ ,  $m^*/m = 0.067$  [18].

Experimental details have been reported elsewhere [1,12,13]. Here, for  $f \leq 50$  GHz, the samples were photoexcited with a digital-frequency-readout microwave generator, with a 1 ppm uncertainty in  $f$  in the cw mode [19]. At higher frequencies, mechanical  $f$  meters with an uncertainty of 0.4% above 100 GHz were used in conjunction with calibration tables to determine  $f$  [20]. Thus,  $f$  is thought to be better characterized below 50 GHz. ESR of DPPH was performed in the immediate vicinity of the 2DES at  $f \leq 10$  GHz using a second digital-frequency-readout microwave source [21]. The  $g$  factor for the unpaired electron undergoing ESR on DPPH is 2.0036, which corresponds to 28.043 GHz/T [22].

Figure 1(a) shows the magnetoresistance  $R_{xx}$  measured in a GaAs/AlGaAs device with microwave excitation at 30 GHz. Also shown is the ESR of DPPH at 2.01 GHz, which marks  $B_f = 2\pi f m^*/e$  for  $f = 30$  GHz and  $m^*/m = 0.067$ . The data of Fig. 1(a) indicate that the ESR field marker coincides neither with a minimum nor with a maximum in the  $R_{xx}$  signal [1]. Figure 1(a) also indicates a strong resistance minimum below  $B_f$ , about  $4/5 B_f$ , which is the  $j = 1$  member of  $B = (4/[4j + 1])B_f$ . These data at 30 GHz also exhibit a deep minimum between  $B_f$  and  $2B_f$ , which is identified here as the possible principal minimum for a two-photon process with a fundamental field  $2B_f$ , expected to form about  $2(4/5 B_f) = 8/5 B_f$ . The data suggest a convergence to  $8/5 B_f$ , as the minimum becomes deeper with increasing microwave power.

Figure 1(b) shows  $R_{xx}$  under photoexcitation at 50 GHz. This panel includes DPPH-ESR field markers which identify  $B_f$ ,  $4/5 B_f$ ,  $B_f/2$ , and  $B_f/2.5$ , for  $f = 50$  GHz. These data show that, at  $\pm B_f$ , there is once again neither a maximum nor a minimum in the  $R_{xx}$ , as in Fig. 1(a). In addition, a zero-resistance state forms about the  $\pm 4/5 B_f$  field marker, and there is neither a maximum nor a minimum in  $R_{xx}$  near the  $\pm B_f/2$  marker [1]. Thus, the data of Fig. 1 indicate that the  $R_{xx}$  maxima do not coincide with  $B_f/j$  [1,2,14,16]. They also confirm the absence of intrinsic sweep-direction dependent hysteretic effects.

Figure 2(a) exhibits  $R_{xx}$  vs  $B^{-1}$  at 50 GHz for several radiation intensities. This plot shows regular-in- $B^{-1}$   $R_{xx}$  oscillations with a number of ‘‘fixed points’’ where  $R_{xx}$  is independent of the microwave power. According to the theory [8], the conductance under radiation should equal the dark conductance at  $B_f/B = j$ . We denote these as integral fixed points (IFP). The experiment also indicates half-integral fixed points (HIFP) in the vicinity of  $B_f/B = j + 1/2$  [12]. The  $B$  measurement of IFP by ESR of DPPH is shown in Fig. 2(b). Here, the ESR of

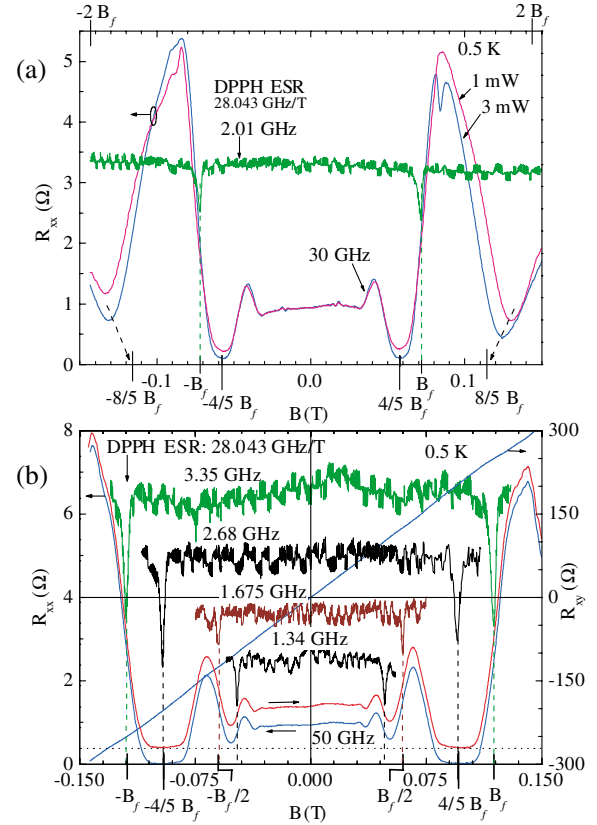


FIG. 1 (color). (a) The magnetoresistance  $R_{xx}$  is plotted vs the magnetic field  $B$  for a GaAs/AlGaAs device under photoexcitation at  $f = 30$  GHz. Also shown is the electron spin resonance (ESR) of diphenyl-picryl-hydrazal (DPPH) at 2.01 GHz, which marks  $B_f = 2\pi f m^*/e$ .  $R_{xx}$  exhibits neither a maximum nor a minimum at  $B_f$ . A deep  $R_{xx}$  minimum between  $B_f < B < 2B_f$  appears to converge to  $2(4/5 B_f) = 8/5 B_f$ , suggestive of a two photon effect. (b)  $R_{xx}$  and  $R_{xy}$  at 50 GHz along with DPPH-ESR field markers for  $B_f$ ,  $4/5 B_f$ ,  $B_f/2$ , and  $B_f/2.5$ . Note the similarity in the up-sweep and down-sweep  $R_{xx}$  curves, and the weak oscillations in  $R_{xy}$ . The up-sweep curve has been offset to improve clarity.

DPPH at  $f_0 = 3.21$  GHz marks the first IFP in the  $R_{xx}$  data of Fig. 2(a). Figures 2(a) and 2(b) indicate that, when  $f_0$  is selected to mark the first IFP,  $f_0/2$  marks a  $B^{-1}$  that is slightly below the second IFP, suggesting a small correction. This correction is attributed here to the observed asymmetry between the resistance increase and the resistance decrease with respect to the dark value. That is, as the  $R_{xx}$  increase under excitation can easily exceed, in magnitude, the  $R_{xx}$  decrease,  $R_{xx}$  peaks tend to span a wider  $B^{-1}$  interval than the  $R_{xx}$  valleys. This tends to relocate the IFP to a slightly higher  $B^{-1}$  value than where the condition  $2\pi f/\omega_c = j$  actually holds true.

Another method for determining the period and the phase of the oscillations involves the application of a half-cycle plot, shown in Fig. 2(c). Typically, the procedure assumes a cosine waveform. Thus, the  $R_{xx}$  maxima and minima are labeled by integers and half integers,

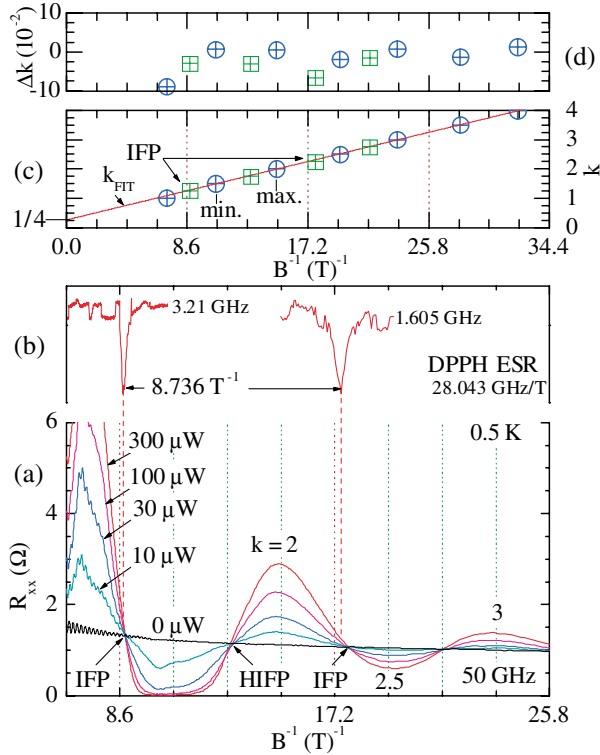


FIG. 2 (color). (a)  $R_{xx}$  is shown vs  $B^{-1}$  for several radiation intensities at 50 GHz. (b) ESR of DPPH for  $f_0 = 3.21$  GHz and  $f_0/2 = 1.605$  GHz. Here,  $f_0$  marks the first integral fixed point (IFP) in (a). The period of the  $R_{xx}$  oscillations,  $8.6 \text{ T}^{-1}$ , appears to be slightly smaller than the spacing of the DPPH-ESR lines. (c) A half-cycle plot of the extrema in (a). A linear fit suggests a  $1/4$ -cycle phase shift. Fixed points, inserted as open squares, were not used for the fit. (d) The residue in  $k$ , i.e.,  $\Delta k = k - k_{\text{FIT}}$ , extracted from (c).

respectively. These labels, denoted here by the index  $k$ , are plotted vs extremal values of  $B^{-1}$ , as in Fig. 2(c). A linear fit,  $k_{\text{FIT}}$ , then serves to determine the slope,  $dk_{\text{FIT}}/dB^{-1} = B_f$ , and the ordinate intercept. Here, in Fig. 2(c), the ordinate intercept at  $1/4$  demonstrates a  $1/4$ -cycle phase shift of  $R_{xx}$  with respect to the assumed (cosine) waveform [13]. The residual difference,  $\Delta k$ , between  $k$  and  $k_{\text{FIT}}$  for the extrema and fixed points, has been shown in Fig. 2(d). Figure 2(d) confirms a small phase distortion, discussed above, at the lowest fixed points. It also confirms that the  $k = 1$   $R_{xx}$  maximum, which tends to be upshifted from  $B_f/B = 3/4$ , is a special case [12] [see also Fig. 3(a)].

There are two parameters in the half-cycle analysis: the intercept and the slope. Yet, the root parameter in the slope is  $m^*$  since  $B_f = 2\pi f m^*/e$ , and  $f$  can be measured. The question then arises whether the measured  $m^*$  agrees with expectations.

In order to obtain a representative sampling of the phase and  $m^*/m$ , we have carried out a half-cycle analysis of a data set obtained over a range  $f$ . For this work, both the extrema and the fixed points were subjected to a

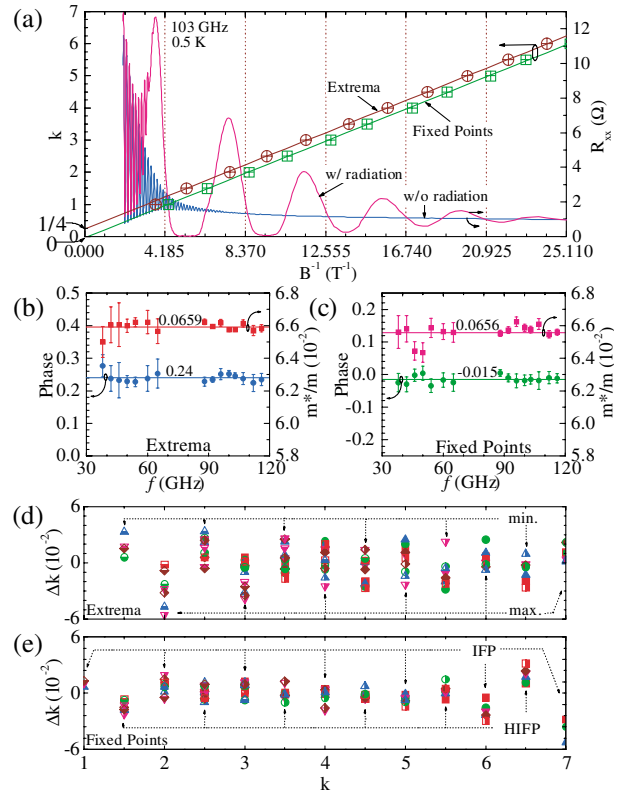


FIG. 3 (color). (a) (right ordinate)  $R_{xx}$  is plotted vs  $B^{-1}$  with (w/) and without (w/o) radiation at 103 GHz. (left ordinate) Half-cycle plots of the extrema and the fixed points in the radiation induced resistance oscillations. The slope of the linear fit is proportional to  $m^*/m$ , while the ordinate intercept measures the phase. (b) The phase and the effective mass ratio,  $m^*/m$ , obtained from linear fits of half-cycle plots of extrema [see (a)] as a function of the frequency. (c) The phase and  $m^*/m$  obtained from linear fits of half-cycle plots of fixed points [see (a)] vs  $f$ . (d) The residue in the extrema labels,  $\Delta k = k - k_{\text{FIT}}$ , is shown as a function of  $k$ , the assigned label, for  $f$  shown in (b). (e) For the fixed points,  $\Delta k$  is shown vs  $k$ , for  $f$  in (c).

separate half-cycle analysis at each frequency, as illustrated in Fig. 3(a) for  $f = 103$  GHz. Since the analysis of the extrema has been discussed above, we note only that an analogous half-cycle analysis of the fixed points involves associating IFP with integers and HIFP with half integers, and plotting the resulting index  $k$  vs  $B^{-1}$ .

A linear least squares fit served to determine the slope and the ordinate intercept of the  $k$  vs  $B^{-1}$  plots, as in Fig. 3(a). The characteristic field,  $B_f$ , and  $m^*/m$  were extracted using  $B_f = dk_{\text{FIT}}/dB^{-1}$ , and  $m^*/m = eB_f/(2\pi f m)$ , where  $m$  is the electron mass. The resulting phase and  $m^*/m$  have been shown in Figs. 3(b) and 3(c). Figure 3(b) shows that the average phase for the extrema is  $0.24 (\pm 0.015)$ , which is  $1/4$  within uncertainty. On the other hand, Fig. 3(c) shows that the average phase for the fixed points is  $-0.015 (\pm 0.012)$ , which is approximately zero. Thus, the phase related results are broadly consistent with resistance minima at  $B_f/B = j + 1/4$ , resistance

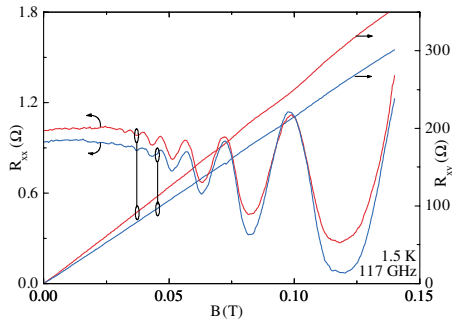


FIG. 4 (color). The periodicity of radiation induced  $R_{xx}$  oscillations appears insensitive to the electron density,  $n$ . Here, increasing the slope of  $R_{xy}$  vs  $B$  corresponds to decreasing  $n$ .

maxima at  $B_f/B = j + 3/4$ , IFP at  $B_f/B = j$ , and HIFP at  $B_f/B = j + 1/2$ , for  $j = 1, 2, 3 \dots$  [12]. The residual difference,  $\Delta k = k - k_{\text{FIT}}$ , for the extrema and fixed points have been shown in Figs. 3(d) and 3(e), respectively. Here, the scatter  $\Delta k$  spans a smaller band in Fig. 3(e) than in Fig. 3(d). Doublet formation on the  $k = 2$  maximum at large  $f$  or low  $T$ , akin to “spin splitting,” has been found to introduce scatter in Fig. 3(d).

So far as the mass ratios are concerned, Fig. 3(b) suggests  $m^*/m = 0.0659 (\pm 0.0004)$ , and Fig. 3(c) indicates that  $m^*/m = 0.0656 (\pm 0.0006)$ . These mass ratios are roughly 2% below the standard value,  $m^*/m = 0.067$  [18], and 1% below our previously reported result,  $m^*/m = 0.0663$  [1]. Here, the difference between the average mass of Figs. 3(b) and 3(c), and the standard value, appears to exceed the resolution limit of this experiment.

Mass corrections can originate from, for example, the polaron effect [23], where an electron polarizes the lattice and creates phonons, and the dressing of the electron by the phonon cloud leads to a mass change, usually a mass increase. An observed mass reduction could be related to some such renormalization effect, if the associated effect is somehow switched off in this context, so that the measurement comes to reflect a bare mass, which then looks like a mass reduction. A theoretical study appears necessary to examine such a possibility. Band nonparabolicity can lead to a dependence of  $m^*/m$  on the electron density,  $n$ , or the Fermi energy. Figure 4 shows, however, that the  $R_{xx}$  oscillation period remains unchanged as  $n$  is varied by  $\approx 15\%$  using the persistent photoeffect.

In summary, we have demonstrated a  $f$ -independent 1/4-cycle phase shift of the extrema in the radiation-induced oscillatory magnetoresistance with respect to the  $\omega/\omega_c = j$  or  $B_f/B = j$  condition for  $j \geq 1$  [4,6,8]. We also find that  $m^*/m$  is 1% smaller than previously reported [1], and about 2% smaller than the standard value [18].

- [1] R.G. Mani, J.H. Smet, K. von Klitzing, V. Narayanamurti, W.B. Johnson, and V. Umansky, *Nature (London)* **420**, 646 (2002).
- [2] M.A. Zudov, R.R. Du, L.N. Pfeiffer, and K.W. West, *Phys. Rev. Lett.* **90**, 046807 (2003).
- [3] R. Fitzgerald, *Phys. Today* **56**, No. 4, 24 (2003).
- [4] V. Ryzhii, *Fiz. Tverd. Tela (Leningrad)* **11**, 2577 (1969) [*Sov. Phys. Solid State* **11**, 2078 (1970)].
- [5] J.C. Phillips, *Solid State Commun.* **127**, 233 (2003).
- [6] A.C. Durst, S. Sachdev, N. Read, and S.M. Girvin, *Phys. Rev. Lett.* **91**, 086803 (2003).
- [7] A.V. Andreev, I.L. Aleiner, and A.J. Millis, *Phys. Rev. Lett.* **91**, 056803 (2003).
- [8] J. Shi and X.C. Xie, *Phys. Rev. Lett.* **91**, 086801 (2003).
- [9] P.W. Anderson and W.F. Brinkman, cond-mat/0302129; K.N. Shrivastava, cond-mat/0302320; S. Mikhailov, cond-mat/0303130; P.H. Rivera and P.A. Schulz, cond-mat/0305019; R. Klesse and F. Merz, cond-mat/0305492; F.S. Bergeret, B. Huckestein, and A.F. Volkov, *Phys. Rev. B* **67**, 241303 (2003); A.A. Koulov and M.E. Raikh, *Phys. Rev. B* **68**, 115324 (2003); V. Ryzhii and R. Suris, *J. Phys. Condens. Matter* **15**, 6855 (2003); X.L. Lei and S.Y. Liu, *Phys. Rev. Lett.* **91**, 226805 (2003); I.A. Dmitriev, A.D. Mirlin, and D.G. Polyakov, *Phys. Rev. Lett.* **91**, 226802 (2003); V. Ryzhii and A. Satou, *J. Phys. Soc. Jpn.* **72**, 2718 (2003).
- [10] *The Quantum Hall Effect*, R.E. Prange and S.M. Girvin (Springer-Verlag, New York, 1990), 2nd ed.
- [11] D.C. Tsui, H. Stormer, and A.C. Gossard, *Phys. Rev. B* **25**, 1405 (1982).
- [12] R.G. Mani *et al.*, cond-mat/0306388.
- [13] R.G. Mani *et al.*, cond-mat/0303034; cond-mat/0305507; cond-mat/0311010; cond-mat/0310474; R.G. Mani, *Physica E (Amsterdam)* (to be published).
- [14] M.A. Zudov, R.R. Du, J.A. Simmons, and J.L. Reno, *Phys. Rev. B* **64**, 201311 (2001).
- [15] Minima about  $B = [4/(4j - 1)]B_f$  would also constitute a 1/4-cycle phase shift, although in the other direction.
- [16] M.A. Zudov, cond-mat/0306508.
- [17] R.G. Mani and K. von Klitzing, *Appl. Phys. Lett.* **64**, 3121 (1994); *Appl. Phys. Lett.* **64**, 1262 (1994); *Z. Phys. B* **92**, 335 (1993); R.G. Mani, *J. Phys. Soc. Jpn.* **65**, 1751 (1996); *Phys. Rev. B* **55**, 15838 (1997).
- [18] S.M. Sze, *Physics of Semiconductor Devices* (Wiley, New York, 1981), p. 850, 2nd ed.; G.E. Stillman, C.M. Wolfe, and J.O. Dimmock, *Solid State Commun.* **7**, 921 (1969).
- [19] 83650B Synthesized Swept-Signal Generator: Agilent Technologies, Palo Alto, CA 94303 ([www.agilent.com](http://www.agilent.com)).
- [20] Series 072 Frequency Meter: Flann Microwave Inc., Bodwin, Cornwall PL31 2QL, UK ([www.flann.com](http://www.flann.com)).
- [21] HP83711A Synthesized CW Generator: Agilent Technologies, Palo Alto, CA 94303 ([www.agilent.com](http://www.agilent.com)).
- [22] R.E. Gerkin *et al.*, *J. Chem. Phys.* **66**, 4166 (1997); F.J. Teran *et al.*, cond-mat/0306634.
- [23] D.M. Larsen, *Phys. Rev.* **135**, A419 (1964).